Journal of Power Sources 196 (2011) 3559–3564

Contents lists available at ScienceDirect

Journal of Power Sources

journal homepage: www.elsevier.com/locate/jpowsour

In-plane gas permeability of proton exchange membrane fuel cell gas diffusion layers

A. Tamayol*, M. Bahrami

School of Engineering Science, Simon Fraser University, BC, Canada

ARTICLE INFO

Article history:
Received 13 September 2010
Received in revised form
10 November 2010
Accepted 22 November 2010
Available online 26 November 2010

Keywords:
PEM fuel cell
In-plane gas permeability
Gas diffusion layer
Blending technique
Fibrous media

ABSTRACT

A new analytical approach is proposed for evaluating the in-plane permeability of gas diffusion layers (GDLs) of proton exchange membrane fuel cells. In this approach, the microstructure of carbon papers is modeled as a combination of equally-sized, equally-spaced fibers parallel and perpendicular to the flow direction. The permeability of the carbon paper is then estimated by a blend of the permeability of the two groups. Several blending techniques are investigated to find an optimum blend through comparisons with experimental data for GDLs. The proposed model captures the trends of experimental data over the entire range of GDL porosity. In addition, a compact relationship is reported that predicts the in-plane permeability of GDL as a function of porosity and the fiber diameter. A blending technique is also successfully adopted to report a closed-form relationship for in-plane permeability of three-directional fibrous materials.

1. Introduction

Proton exchange membrane fuel cells (PEMFCs) have shown the potential to be commercialized as power sources in automotive, electronic, portable, and stationary applications [1]. The membrane electrode assembly (MEA), the heart of a PEMFC, is composed of a membrane loaded by catalyst layers on each side and is sandwiched between two porous layers named gas diffusion layers (GDLs) [1]. In addition to mechanical support of the membrane, GDL allows transport of reactants, products, and electrons from the bipolar plate towards the catalyst layer and vice versa. Therefore, thermophysical properties of GDLs such as gas and water permeabilities, thermal, and electrical conductivities affect the PEMFC performance and reliability. Transport of reactants in the through-plane direction is a diffusive mechanism rather than a convective mechanism; thus, the only pressure driven mass transfer occurs in the in-plane direction [2]. Several theoretical and experimental studies have shown that the in-plane permeability of GDLs is a key parameter in optimization of PEMFCs performance [3–8].

The applied pressure for sealing a PEMFC changes the GDL thickness and its porosity; this affects the transport properties of the GDL. For example, the gas permeability reduces as a result of the GDL compression while the thermal and electrical conductivities increase. As such, a trade off exists in the design and optimization process of MEAs [9–11]. Therefore, having a model that can predict the in-plane permeability of GDLs as a function of porosity is valuable in the design of high performance PEMFCs.

There are few experimental studies available in the literature that reported the permeability of GDLs [12–16]. Ihonen et al. [14] showed that a reverse relationship exists between the in-plane permeability and compression. Recently, Feser et al. [2] studied the effects of compression and reported the in-plane gas permeability as a function of porosity for a carbon cloth, a non-woven carbon fiber GDL, and a carbon paper. In a similar work, Gostick et al. [16] measured the permeability of several commercial GDLs under various compressive loads and reported the in-plane permeability as a function of porosity. More details of the experimental studies can be found in Ref. [17].

She et al. [18] employed a fractal permeability model that accounted for the microstructures of GDLs in terms of two fractal dimensions and proposed a relationship for permeability as a function of tortuosity, fractal dimensions, pore area fractal dimensions, pore size distribution, and effective porosity. Their model, however, requires several geometrical parameters (e.g., fractal parameters) that should be known beforehand. Lattice Boltzmann simulations of gas flow through several random fibrous structures were carried out by Vandoormaal and Pharoah [19] over the porosity range of $0.6 < \varepsilon < 0.8$. They reported numerical results for different fiber orientations which were an order of magnitude different in a constant porosity. Based on the permeability values for structures with

* Corresponding author at: Mechatronic Systems Engineering, Simon Fraser University, #4300, 250 – 13450 102nd Avenue, Surrey, BC, Canada V3T0A3. Tel.: +1 778 782 8587; fax: +1 778 782 7514.
E-mail addresses: ali_tamayol@sfu.ca, ata42@sfu.ca (A. Tamayol).

0378-7753/$ – see front matter © 2010 Elsevier B.V. All rights reserved.
doi:10.1016/j.jpowsour.2010.11.109

Nomenclature

d	fiber diameter (m)
GDL	gas diffusion layer
K	viscous permeability (m^2)
K_{eq}	equivalent permeability of the mixture (m^2)
P	pressure (Pa)
S	distance between centers of adjacent fibers (m)
U_D	volume-averaged superficial velocity ($m\,s^{-1}$)

Greek symbols

ε	porosity
μ	fluid viscosity ($N\,s\,m^{-2}$)
φ	solid volume fraction, $\varphi = 1 - \varepsilon$
φ'	dimensionless parameter in Eq. (3), $\varphi' = \pi/4(1-\varepsilon)$

Subscript

par	parallel to flow direction
norm	normal to flow direction
tot	total
eq	equivalent

mixed orientations, they proposed two correlations for in-plane and through-plane permeabilities of the considered structures which were not compared with experimental data of actual GDLs.

Our literature review indicates the need for a general model that can accurately predict the in-plane permeability of GDLs, and its trends as a function of porosity and fibers diameter. Therefore, the objectives of the present work are to:

- Develop and verify a comprehensive analytical model that can predict the in-plane gas permeability of GDLs and other complex fibrous structures that captures the trends observed in experimental data.
- Investigate the effects of relevant geometrical parameters involved and identify the controlling parameters.

In this study, a novel approach is proposed for studying gas flow through GDLs where the porous medium is assumed as a combination of fibers normal and parallel to the flow direction. We then propose that a blend of the normal and parallel permeabilities of unidirectional fibers can provide an estimate for the in-plane permeability of GDLs. The fraction of fibers in each direction is evaluated from a simplified ordered geometry structure representing the microstructure of carbon paper. Several blending techniques are compared against experimental data collected from different sources. It is observed that the volume weighted blend is a better choice for the in-plane permeability of GDLs. Moreover, a compact relationship is presented for determining the in-plane permeability of GDLs as a function of porosity and fiber diameter. The applicability of blending technique for predicting in-plane permeability of fibrous materials with three-directional microstructure is also investigated. The volume-weighted resistivity scheme captures the trend of experimental data for permeability of hydrogels, metallic rods, metalfoams, and glass wool.

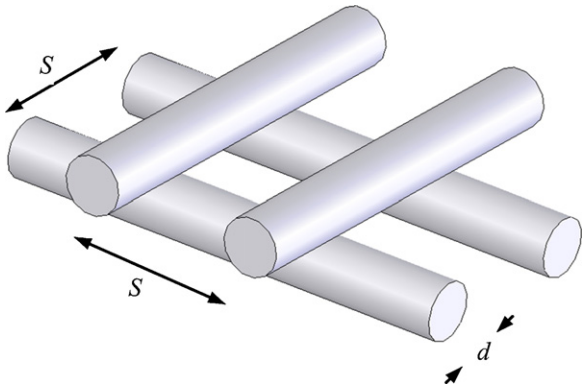

Fig. 2. Proposed periodic geometry for modeling GDLs.

2. Model development

Permeability, K, can be interpreted as a measure of the flow conductance of the porous material and is defined using Darcy equation [20]:

$$-\frac{dP}{dx} = \frac{\mu}{K} U_D \tag{1}$$

where U_D is the volume averaged velocity through porous media, μ is viscosity and dP/dx is the pressure difference between two points in the flow-field. Darcy equation with the form of Eq. (1) is valid for incompressible, steady, constant properties, single-phase (no-surface tension forces), and low Reynolds number flows. As such, the same assumptions are considered in the present analysis.

There are different types of GDLs including carbon paper type, carbon fiber cloth, and wet-/dry-laid papers [19]. The carbon paper type is the focus of the present study. An SEM image of Toray carbon paper is shown in Fig. 1. Gas permeability of such fibrous structures depends on several factors including: porosity, fibers size and distribution. In carbon papers, the axes of fibers are located on parallel planes with random distribution and orientation, see Fig. 1. Therefore, the geometry shown in Fig. 2 can be assumed as an idealized representation of the GDLs. The porosity of the ordered structure is related to the distance between the centers of adjacent fibers, S,

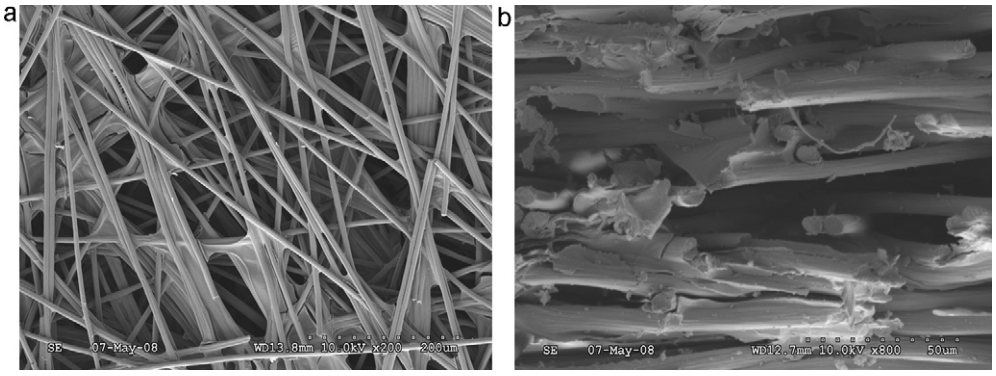

Fig. 1. SEM image of Toray 90 carbon paper: (a) top view; (b) side view.

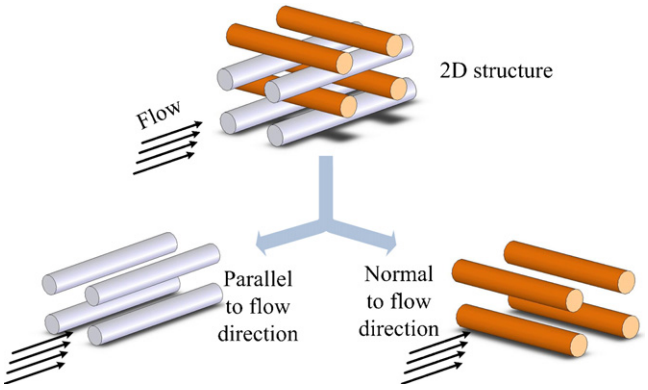

Fig. 3. Summary of the blending technique concept for 2D fibrous structures (GDLs).

and the fibers diameter d:

$$\varepsilon = 1 - \frac{\pi}{4}\frac{d}{S} \tag{2}$$

Following Jackson and James [21], the carbon paper is modeled as a mixture of fibers parallel and normal to flow direction with solid volume fractions of φ_{par} and φ_{norm}, respectively; for the geometry shown in Fig. 2, $\varphi_{par} = \varphi_{norm} = \varphi_{tot}/2$. As such, it is expected that the equivalent permeability, $K_{eq}(\varphi)$, is related to the permeability of each component; the concept of blending technique is shown in Fig. 3. It should be noted that there is no concrete rules for estimating the mixtures permeability. Blending techniques have been successfully employed to estimate the permeability of fibrous mixtures such as hydrogels [21], fibers with different sizes [22], and fibers with different charges [23,24]. However, to our best knowledge, the application of blending techniques to planar structures such as GDL is novel.

Different blending rules, originally developed for different applications, are rewritten for a mixture of fibers with different orientations and are listed in Table 1. One difference among the blending schemes is the way the interactions between a fiber and its neighbours are considered. The other difference is the way each fiber category affects the overall pressure drop. The volume-weighted permeability is based on the assumption that the two types of fibers occupied separate, parallel phases in a slab of fibrous material [24]. In other words, the volume-weighted permeability model considers each fiber category as parallel flow resistors. The weighted resistivity schemes assume that the two fiber categories act similar to flow resistors in series, i.e., the resistivity based methods consider the fibrous material as combination of various layers in series. The geometric mean scheme is a purely mathematical blend.

To estimate the mixture permeability from using the equations listed in Table 1, one needs to know the permeability of the fibers in both normal and parallel directions.

Table 1
A summary of various blending methods investigated for estimation of in-plane permeability of planar structures (GDLs).

Blending model	Relationship
Volume-weighted resistivity	$\frac{1}{K_{eq}(\varphi)} = \frac{\varphi_{par}}{\varphi}\frac{1}{K_{par}(\varphi)} + \frac{\varphi_{norm}}{\varphi}\frac{1}{K_{norm}(\varphi)}$
Unweighted resistivity	$\frac{1}{K_{eq}(\varphi)} = \frac{1}{K_{par}(\varphi_{par})} + \frac{1}{K_{norm}(\varphi_{norm})}$
Volume weighted permeability	$K_{eq}(\varphi) = \frac{\varphi_{par}}{\varphi}K_{par}(\varphi) + \frac{\varphi_{norm}}{\varphi}K_{norm}(\varphi)$
Geometric mean	$K_{eq}(\varphi) = (K_{par}(\varphi))^{\varphi_{par}/\varphi}(K_{norm}(\varphi))^{\varphi_{norm}/\varphi}$

$\varphi_{par} = \varphi_{norm} = \frac{\varphi_{tot}}{2}$

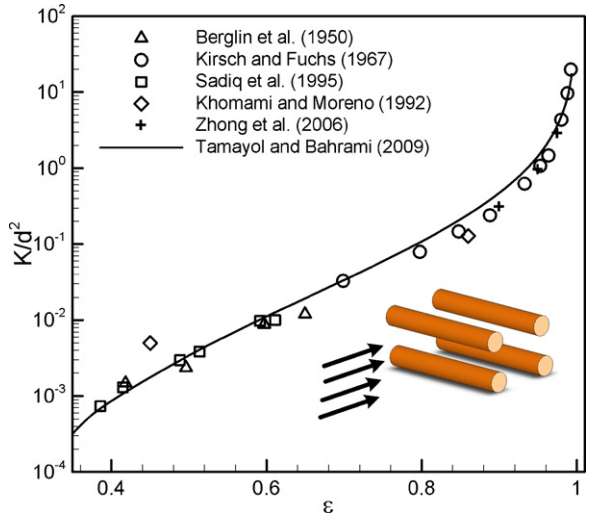

Fig. 4. Comparison of Eq. (3) with experimental data for normal permeability of unidirectional fibers [25].

2.1. Normal permeability

Recently, Tamayol and Bahrami [25–27] have analytically studied the normal and parallel permeabilities of ordered arrangements of unidirectional fibers. In Ref. [25], assuming a parabolic velocity profile within square arrangements of equally-sized fibers and integrating the continuity and momentum equations, a closed form analytical solution has been reported for the pressure drop and permeability:

$$K_{norm} = \left\{ \frac{12(\sqrt{\varphi'}-1)}{\varphi'\sqrt{\varphi'}}\left[\frac{2-g(\varepsilon)}{2}\right] + \frac{18+12(\varphi'-1)}{\sqrt{\varphi'(1-\varphi')^2}} + \frac{18\sqrt{\varphi'}\left[\tan^{-1}\left(\frac{1}{\sqrt{\varphi'-1}}\right)+\frac{\pi}{2}\right]}{(\varphi'-1)^{\frac{5}{2}}} \right\}^{-1} d^2,$$

$$\varphi' = \frac{\pi}{4(1-\varepsilon)}, \quad g(\varepsilon) = 1.274\varepsilon - 0.274 \tag{3}$$

Eq. (3) is compared with experimental data for normal permeability of unidirectional fibers [28–32] in Fig. 4. It can be seen that the model of [25] is in a reasonable agreement with experimental data over the entire range of porosity. As such, Eq. (3) is used to calculate the permeability of fibers normal to flow direction in the blending models.

2.2. Parallel permeability

Tamayol and Bahrami [26] studied steady, incompressible, and fully-developed flow parallel to axes of mono-disperse fibers in several ordered arrays of cylinders. They started from general solution of the Poisson's equation and using point matching technique reported closed-form analytical solutions for velocity distribution in the considered geometries including: square, staggered, and hexagonal arrays of fiber. Their solution for parallel permeability of square fiber arrangements is:

$$K_{par} = \frac{d^2}{16\varphi}\left[-1.479 - \ln\varphi + 2\varphi - \frac{\varphi^2}{2} - 0.0186\varphi^4\right] \tag{4}$$

where φ is the fiber volume fraction, $\varphi = 1 - \varepsilon$. In Fig. 5, this model is compared with experimental and numerical data found in the literature [26,33–35]. As shown in Fig. 5, Eq. (4) is also in good agreement with the collected data over the entire range of porosity.

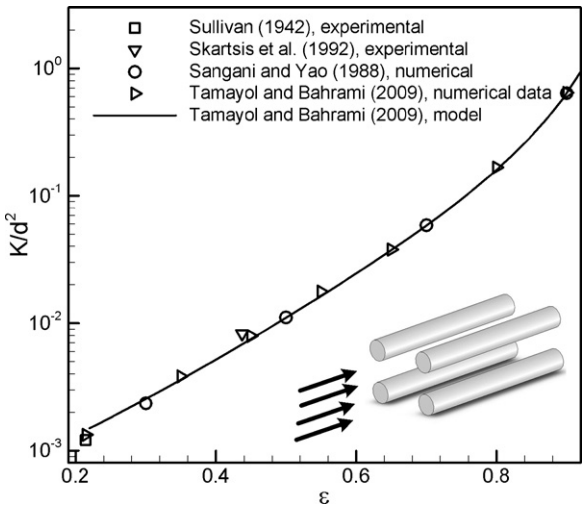

Fig. 5. Comparison of Eq. (4) with experimental data for parallel permeability of unidirectional fibers [26].

Therefore, Eq. (4) is employed to estimate the parallel permeability in the blending rules.

2.3. Comparison of different blending rules for planar structures (GDLs)

The blending models listed in Table 1 combined with normal and parallel permeabilities presented by Eqs. (3) and (4) are used to calculate the permeability of the geometry shown in Fig. 2. In the considered geometry, 50% of fibers are parallel and 50% of fibers are normal to flow direction, i.e., $\varphi_{par} = \varphi_{norm} = \varphi_{tot}/2$. The calculated results from different blending rules are plotted in Fig. 6. It can be seen that the blending rules fall between normal and parallel permeabilities of square arrays of cylinders and at high porosities, $\varepsilon > 0.7$, there is a small difference between different models.

Our analysis showed that the volume weighted permeability scheme is in better agreement with experimental data in lower porosities, $\varepsilon < 0.7$. This blending model is written in the following easy-to-use form:

$$K(\varepsilon, d) = \exp\left(\frac{-12.95 + 13.9\varepsilon}{1 + 1.57\varepsilon - 2.22\varepsilon^2}\right) d^2 \quad (5)$$

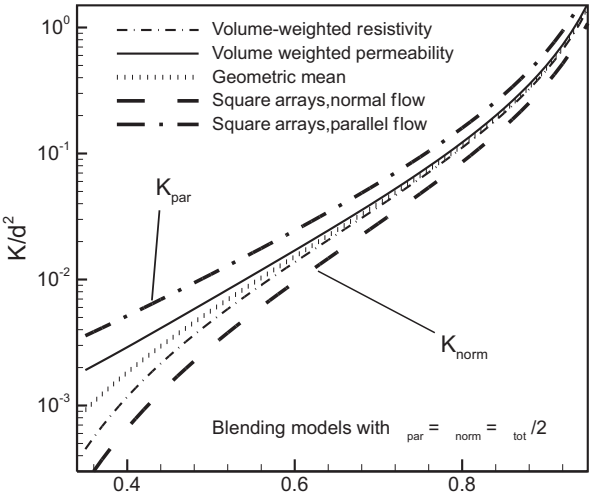

Fig. 6. Comparison of different blending models with the bounds for $\varphi_{par} = \varphi_{norm} = \varphi_{tot}/2$.

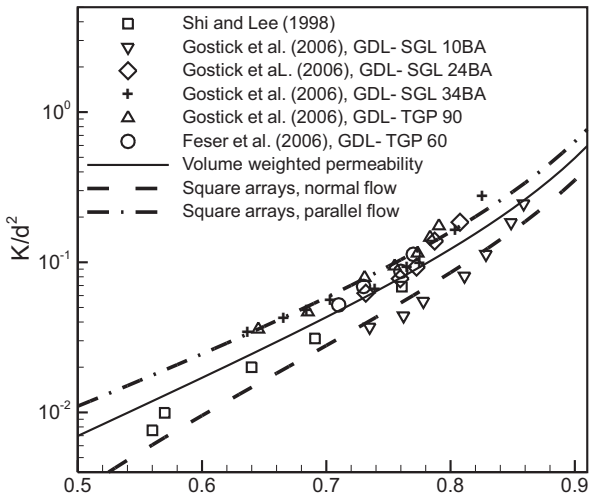

Fig. 7. Comparison of the proposed blending model with the experimental data for planar structures; experimental data from Feser et al. [2] and Gostick et al. [16] are for various types of GDLs.

This relationship is only a function of porosity and fiber diameter. Comparison of Eq. (5) with experimental data is presented in the following sections.

3. Comparison with experimental data

The blending model is compared with experimental results of Gostick et al. [16] and Feser et al. [2] for a variety of carbon paper GDLs in Fig. 7. In addition, to increase the porosity range of experimental data, the results reported by Shi and Lee [36] for composite fabrication application are included. The composite reinforcement mats have a similar microstructure to GDLs [37]. The permeability values are non-dimensionalized using the fiber diameters reported in the abovementioned studies.

Fig. 7 shows that the volume weighted permeability method predicts the trends of experimental data over a wide range of porosity.

As such, it can be concluded that a parallel network comprised of the flow resistors for fibers parallel and normal to flow directions, captures the overall flow resistance accurately.

Most of the experimental data fall between the normal and parallel permeabilities of the square arrangement of fibers. Therefore, normal and parallel permeability of unidirectional fibers can be viewed as upper and lower bounds for the in-plane gas permeability of fibrous porous media such as GDLs, i.e., the permeability of fibers with mixed orientations is bounded by the two limiting cases when all of the fibers are oriented either parallel or normal to the flow direction. This is in line with the previous observations of Tomadakis and Robertson [37] and Tamayol and Bahrami [25].

Our analysis suggests that in-plane permeability is proportional to the fibers diameter squared; this is in line with other theoretical models listed in Table 2. The experimental data for various materials with different diameters, non-dimensionalized using d^2 in Fig. 7, follows our proposed relationship, which verifies existence of this proportionality.

4. Comparison with other existing models

In Fig. 8, the present model, Eq. (5), and the collected experimental data are compared against the correlations reported by Tomadakis and Sotirchos [40] and Van Doormaal and Pharoah [19]; see Table 2 for more details. The model of Tomadakis and Sotirchos (TS) [38] was based on the analogy between electrical and flow

Table 2
A summary of existing models for in-plane permeability of planar structures.

Reference	Relationships	Remarks
[38]	$K = \frac{\varepsilon}{8(\ln\varepsilon)^2}\left(\frac{(\varepsilon-\varepsilon_p)^{(\alpha+2)}}{(1-\varepsilon_p)^{\alpha}[(\alpha+1)\varepsilon-\varepsilon_p]^2}\right)d^2, \quad \varepsilon_p = 0.11, \quad \alpha = 0.521$	• Based on the analogy between electrical and flow conductions • Accurate only for $\varepsilon < 0.8$ • Developed for over lapping fibers
[19]	$K = 0.065\frac{\varepsilon^{3.6}}{1-\varepsilon}d^2$	• Based on curve fit of numerical results • Accurate only for $0.6 < \varepsilon < 0.8$

conductions. This model was originally developed for permeability of randomly distributed overlapping fibers in composite reinforcements [37]. It can be seen that both Eq. (5) and the model of [38] predict the trends of experimental data over the low to medium range of porosity. However, TS model [38] overpredicts the data in high porosities, $\varepsilon < 0.8$, while Eq. (5) is in agreement with the experimental data over the entire range of porosity.

5. Permeability of three-directional fibrous structures

To further investigate application of blending techniques for estimating permeability of fibrous media with complex but non-planar microstructure, a similar analysis has been conducted for three-directional [37] fibrous structures with random distribution and orientation of fibers in the space. Following Jackson and James [21] the complex geometry of is modeled with the simple cubic (SC) arrangement shown in Fig. 9. In the SC structure, 1/3 of fibers are parallel and 2/3 of fibers are normal to flow direction see Fig. 10, i.e., $\varphi_{par} = \varphi_{tot}/3$, $\varphi_{norm} = 2\varphi_{tot}/3$. The volume-weighted resistivity scheme is in a reasonable agreement with experimental data and is written in the following compact form:

$$K(\varepsilon, d) = \exp\left(\frac{-43.25 + 46.6\varepsilon}{1 + 10.56\varepsilon - 10.5\varepsilon^2}\right)d^2 \quad (6)$$

In Fig. 11, the proposed model is compared with the experimental values of permeability of hydrogels, metallic rods, metalfoams, and glass wool [39–44]. Moreover, a selection of other existing models [21,38] is included in the figure. It can be seen that the blending technique is the only model that captures the trend of experimental data over the entire range of porosity.

6. Conclusions

A novel analytical model was developed for the in-plane permeability of gas diffusion layers as a function of porosity and fiber diameter. In this approach, the porous medium was considered as a mixture of fibers parallel and normal to flow directions. Then, the permeability of the mixture was modeled as a blend of the permeabilities of its components. The normal and parallel fiber permeabilities were evaluated from our previous analytical studies for flow through square arrays of fibers. To find the fraction of each fibers category, an ordered equally-sized, equally spaced planar microstructure was assumed. The highlights of the present study can be summarized as:

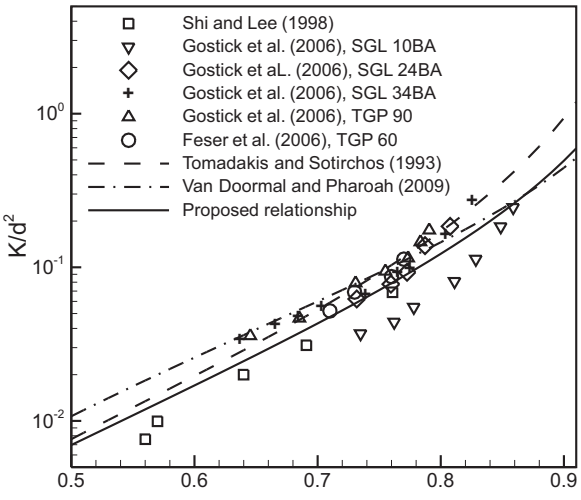

Fig. 8. Comparison of present model with other existing correlations for the in-plane permeability of fiber mats.

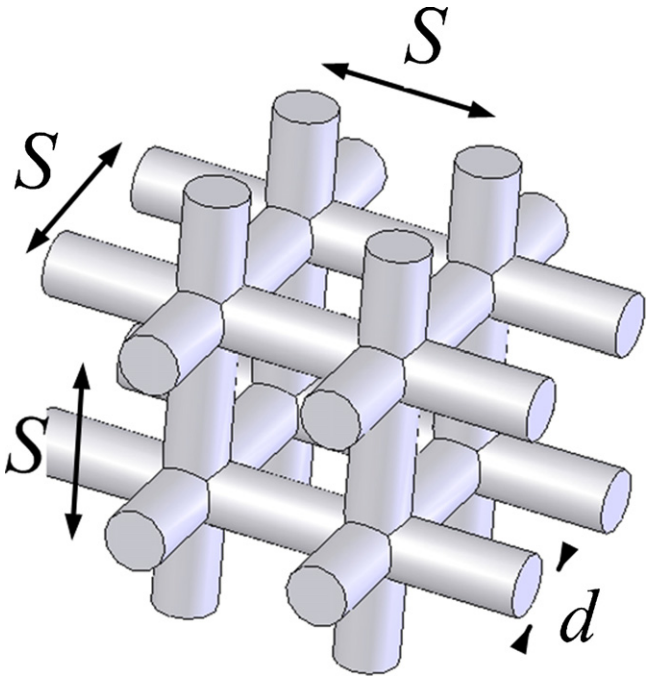

Fig. 9. Proposed periodic geometry for modeling 3D (non-planar) fibrous structures.

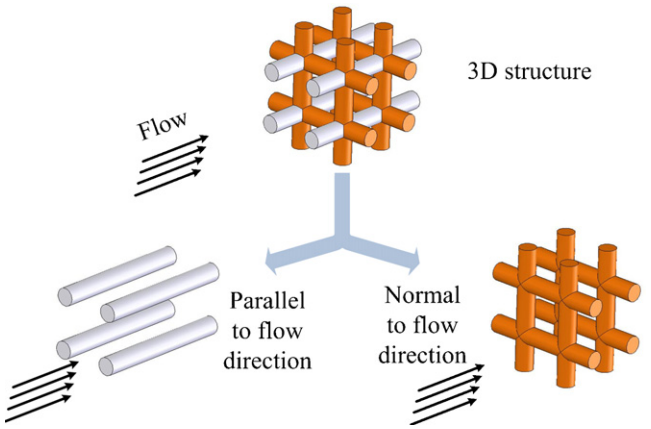

Fig. 10. The blending technique concept for 3D fibrous structures.

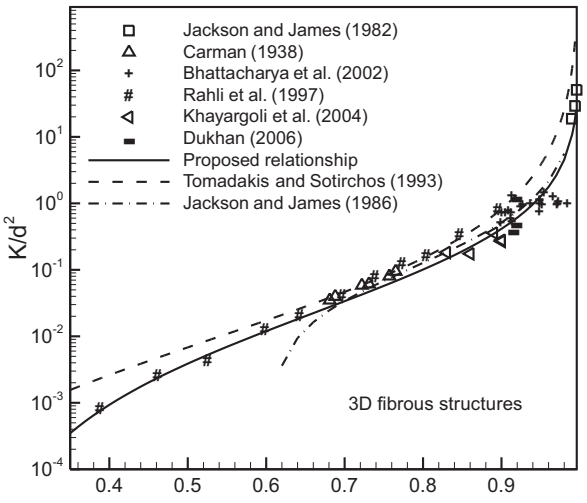

Fig. 11. Comparison of present model and other existing correlations with experimental data for the in-plane permeability of three-directional fibrous structures.

- Normal and parallel permeability of the fibers provides bounds for the permeability GDLs, see Fig. 7.
- GDLs can be treated as a combination of fibers with different orientations. Therefore, the proposed approach may be used for predicting other transport properties.
- Permeability of GDLs is directly proportional to its porosity and the fibers diameter squared.

Employing the blending rules, a compact relationship was proposed for gas in-plane permeability of GDLs which was a function of the porosity and fibers diameter. The model can be used to guide the design and optimization of PEMFCs, and can be readily implemented into fuel cell models that require specification of the in-plane gas permeability of the GDL.

The blending approach with the volume-weighted resistivity scheme captures the trends of values for in-plane permeability of three-directional fibrous materials such as hydrogels, metallic rods, metalfoams, and glass wool.

Acknowledgement

The authors gratefully acknowledge the financial support of the Natural Sciences and Engineering Research Council of Canada (NSERC).

References

[1] A. Faghri, Z. Guo, Int. J. Heat Mass Transfer 48 (2005) 3891–3920.
[2] J.P. Feser, A.K. Prasad, S.G. Advani, J. Power Sources 161 (2006) 1226–1231.
[3] J.P. Feser, A.K. Prasad, S.G. Advani, J. Power Sources 162 (2006) 404–412.
[4] J. Pharaoh, J. Power Sources 144 (2005) 77–82.
[5] M. Mathias, J. Roth, J. Fleming, W. Lehnert, in: W. Viestich, H.A. Gasteiger, A. Lamm (Eds.), Fuel Cell Technology and Applications, vol. 3, John Wiley & Sons Ltd., 2003.
[6] T.V. Nguyen, J. Electrochem. Soc. 143 (1996) L103–L105.
[7] G. Hu, J. Fan, S. Chen, Y. Liu, K. Cen, J. Power Sources 136 (2004) 1–9.
[8] W. Sun, B. Peppley, K. Karan, J. Power Sources 144 (2005) 42–53.
[9] J. Ge, A. Higier, H. Liu, J. Power Sources 159 (2006) 922–927.
[10] P.T. Nguyen, T. Berning, N. Djilali, J. Power Sources 130 (2004) 149–157.
[11] T. Berning, N. Djilali, J. Electrochem. Soc. 150 (2003) A1589–A1598.
[12] V. Gurau, M.J. Bluemle, E.S. De Castro, Y. Tsou, T.A. Zawodzinski Jr., J. Adin Mann Jr., J. Power Sources 165 (2007) 793–802.
[13] M. Williams, R. Kuntz, J. Fenton, J. Electrochem. Soc. 151 (2004) 1617–1627.
[14] J. Ihonen, M. Mikkola, G. Lindbergh, J. Electrochem. Soc. 151 (2004) 1152–1161.
[15] B. Mueller, T.A. Zawodzinski, J. Bauman, F. Uribe, S. Gottesfeld, in: T.F. Fuller, S. Gottesfeld (Eds.), Proceedings of the Second International Symposium on Proton Conducting Membrane Fuel Cells, 1999, pp. 1–9.
[16] J.T. Gostick, M.W. Fowler, M.D. Pritzker, M.A. Ioannidis, L.M. Behra, J. Power Sources 162 (2006) 228–238.
[17] L. Cindrella, A.M. Kannana, J.F. Lina, K. Saminathana, Y. Hoc, C.W. Lind, J. Wertze, J. Power Sources 194 (2009) 146–160.
[18] Y. Shi, J.S. Xiao, M. Pan, R.Z. Yuan, J. Power Sources 160 (2006) 277–283.
[19] M.A. Van Doormaal, J.G. Pharoah, Int. J. Numer. Meth. Fluids 59 (2009) 75–89.
[20] M. Kaviany, Principles of Heat Transfer in Porous Media, Springer-Verlag, 1992.
[21] G.W. Jackson, D.F. James, Can. J. Chem. Eng. 64 (1986) 364–374.
[22] D.S. Clauge, R.J. Philips, Phys. Fluids 9 (1997) 1562–1572.
[23] S.R. Eisenberg, A.J. Grodzinsky, PhysicoChem. Hydrodyn. 10 (1988) 517–539.
[24] K.J. Mattern, W.M. Deen, AIChE 54 (2008) 32–41.
[25] A. Tamayol, M. Bahrami, Int. J. Heat Mass Transfer 52 (2009) 3691–3701.
[26] A. Tamayol, M. Bahrami, Parallel flow in ordered fibrous structures: An analytical approach, J. Fluid Eng. 132 (2010) 114502–114507.
[27] A. Tamayol, M. Bahrami, Scaling laws for transverse permeability of fibrous porous media, Physical Review E, in press.
[28] W.H. Zhong, I.G. Currie, D.F. James, Exp. Fluids 40 (2006) 119–126.
[29] O.P. Bergelin, G.A. Brown, H.L. Hull, F.W. Sullivan, J. Heat Transfer 72 (1950) 881–888.
[30] A.A. Kirsch, N.A. Fuchs, Ann. Occup. Hygiene 10 (1967) 23–30.
[31] T.A.K. Sadiq, S.G. Advani, R.S. Parnas, Int. J. Multiphase Flow 21 (1995) 755–774.
[32] B. Khomami, L.D. Moreno, Rheol. Acta 36 (1997) 367–383.
[33] R.R. Sullivan, J. Appl. Phys. 13 (1942) 725–730.
[34] L. Skartsis, B. Khomami, J.L. Kardos, Polym. Eng. Sci. 32 (1992) 231–239.
[35] A.S. Sangani, C. Yao, Phys. Fluids 31 (1988) 2435–2444.
[36] C.H. Shih, L.J. Lee, Polym. Compos. 19 (1998) 626–639.
[37] M.M. Tomadakis, T. Robertson, J. Compos. Mater. 39 (2005) 163–188.
[38] M.M. Tomadakis, S.V. Sotirchos, J. Chem. Phys. 98 (1993) 616–626.
[39] P.C. Carman, J. Soc. Chem. Ind. 57 (1937) 225–234.
[40] D.F. James, G.W. Jackson, Biorhelogy 19 (1982) 317–330.
[41] O. Rahli, L. Tadrist, M. Miscevic, R. Santini, J. Fluids Eng. 119 (1997) 188–192.
[42] A. Bhattacharya, V.V. Calmidi, R.L. Mahajan, Int. J. Heat Mass Transfer 45 (2002) 1017–1031.
[43] P. Khayargoli, V. Loya, L.P. Lefebvre, M. Medraj, Proc. CSME (2004) 220–228.
[44] N. Dukhan, Exp. Fluids 41 (2006) 665–672.